The fingerprint of climate trends on European crop yields

Frances C. Moore[a,b,1] and David B. Lobell[b,c]

[a]Emmett Interdisciplinary Program in Environment and Resources, [b]Center for Food Security and the Environment, and [c]Department of Environmental Earth System Science, Stanford University, Stanford, CA 94305

Edited by Benjamin D. Santer, Lawrence Livermore National Laboratory, Livermore, CA, and approved January 9, 2015 (received for review May 23, 2014)

Europe has experienced a stagnation of some crop yields since the early 1990s as well as statistically significant warming during the growing season. Although it has been argued that these two are causally connected, no previous studies have formally attributed long-term yield trends to a changing climate. Here, we present two statistical tests based on the distinctive spatial pattern of climate change impacts and adaptation, and explore their power under a range of parameter values. We show that statistical power for the identification of climate change impacts is high in many settings, but that power for identifying adaptation is almost always low. Applying these tests to European agriculture, we find evidence that long-term temperature and precipitation trends since 1989 have reduced continent-wide wheat and barley yields by 2.5% and 3.8%, respectively, and have slightly increased maize and sugar beet yields. These averages disguise large heterogeneity across the continent, with regions around the Mediterranean experiencing significant adverse impacts on most crops. This result means that climate trends can account for ∼10% of the stagnation in European wheat and barley yields, with likely explanations for the remainder including changes in agriculture and environmental policies.

climate change | agriculture | attribution | Europe | adaptation

Europe has experienced a stagnation of yields for some crops, particularly wheat and barley, with a plateau since the early to mid-1990s (Fig. 1*A*) (1, 2). Explanations for this stagnation have focused on changing agricultural policy and, to a lesser extent, on shifting climate patterns (3, 4). Much of Europe saw the introduction of more stringent environmental policies during the 1990s, as well as the decoupling of subsidy payments from farm production in the European Union, both of which would be expected to lower the intensity of cereal production (5, 6). In addition, warming trends in the region have been large relative to natural variability and could be expected to negatively affect yields, particularly in southern Europe (*SI Appendix*, Fig. S1) (7, 8).

Existing empirical evidence for either explanation is typically weak, taking the form of coincidence in the direction and timing of expected climate or policy effects with yield trends, so the relative importance of these mechanisms has not been rigorously demonstrated (3, 9). More persuasive detection and attribution studies instead identify impacts using a distinctive spatial pattern of trends associated with climate change forcing (10, 11). Because the spatial distribution of long-term trends is less likely to be correlated with other variables, these studies are better able to make a case for climate's causal effect on the outcome of interest. Fig. 1 *B*–*E* shows the observed trends in yields of wheat, maize, barley, and sugar beet in Europe between 1989 and 2009. Fig. 1 *F*–*I* shows the trends in yield that would have been expected given observed changes in growing-season temperature and precipitation and the sensitivity of crops to those changes (8). Observed trends are both more positive and more spatially heterogeneous than the predicted trends, which would be expected given that the latter do not include the effects of technological improvements or of changing economic or policy conditions. Nevertheless, formal statistical tests can reveal whether or not the distinctive pattern, or fingerprint, of climate trend impacts is embedded within the observed pattern of long-term yield trends.

Formal detection of a climate change signal and the attribution of that signal to anthropogenic greenhouse gas emissions has been successful in many physical and some biological systems (10–12). However, few studies have attributed changing yield pattern to climate trends. This analysis is complicated by two factors. First, the expected response of agriculture to a given temperature or precipitation forcing is determined by an imperfectly known response function. This response uncertainty must be accounted for in determining whether or not climate change has had a statistically discernable impact. Second, farmers may or may not be adapting to the climate change they have experienced, creating additional uncertainty in the expected response of agriculture to climate forcing (13). This potential for adaptation means there are two response functions relevant to the detection (and prediction) of climate change impacts: the short-run response function that includes limited or no adaptation, and the long-run response function that includes full adaptation (8).

In this paper, we first develop two general statistical tests that can be applied to the detection of impacts and adaptation in any managed system affected by climate change and report the power of these tests under a range of parameter values. We then apply these tests to Europe to determine whether climate trends have affected yields and, if so, to what extent these impacts can explain the stagnation of European cereal yields.

Statistical Tests for Climate Change Impacts and Adaptation

Here, we present two formal statistical tests, the first designed to distinguish a system affected by climate trends from one not affected, and the second to distinguish a system adapting rapidly from one not adapting. Both tests rely on knowing the climate response function, namely how the outcome of interest y should respond to changes in climate variables w, either including adaptation [the long-run response function, $y = f_{LR}(w)$] or not

Significance

Agriculture is one of the economic sectors most exposed to climate change impacts, but few studies have statistically connected long-term changes in temperature and rainfall with yields. Doing so in Europe is particularly important because yields of wheat and barley have plateaued since the early 1990s and climate change has been suggested as a cause of this stagnation. Here, we show that the impact of climate trends can be detected in the pattern of long-term yield trends in Europe. Although impacts have been large in some areas, the aggregate effect across the continent has been modest. Climate trends can explain 10% of the slowdown in wheat and barley yields, with changes in agriculture and environmental policies possibly responsible for the remainder.

Author contributions: F.C.M. and D.B.L. designed research; F.C.M. performed research; F.C.M. analyzed data; and F.C.M. and D.B.L. wrote the paper.

The authors declare no conflict of interest.

This article is a PNAS Direct Submission.

[1]To whom correspondence should be addressed. Email: fcmoore@stanford.edu.

This article contains supporting information online at www.pnas.org/lookup/suppl/doi:10.1073/pnas.1409606112/-/DCSupplemental.

including adaptation [the short-run response function, $y = f_{SR}(w)$]. These response functions could be determined statistically (the approach in this paper), using a process-based model, or from known theoretical relationships. In many cases, the response functions may be nonlinear and in most cases will contain uncertain parameters.

As in other detection and attribution studies, these tests rely on comparing the spatial pattern of long-term trends in the variable of interest to what would be expected given the observed long-term trends in climate (14). Three linear time trends are calculated for each region i: the observed trend, the predicted long-run trend, and the predicted short-run trend:

$$y_{it} = \alpha_0 + Observed\_Trend_i * t + \varepsilon_{it},$$

$$f_{LR}(w_{it}) = \alpha_1 + Predicted\_Trend\_LR_i * t + \varepsilon_{it},$$

$$f_{SR}(w_{it}) = \alpha_2 + Predicted\_Trend\_SR_i * t + \varepsilon_{it}.$$

The region-specific trends $Predicted\_Trend\_LR_i$ and $Predicted\_Trend\_SR_i$ give a distinctive spatial pattern of the expected climate change impact that can be compared with the observed trends. The climate variables used in this paper (w_{it}) are the average growing season temperature and rainfall in subnational region i in year t.

Our first test for the detection of climate change impacts (test 1) is based on the regression:

$$Observed\_Trend_i = \beta_0 + \beta_1 Predicted\_Trend_i + \varepsilon_i, \quad [1]$$

where $Predicted\_Trend_i$ could be either from the short- or long-run response function. Here, we report results using the long-run response function because it includes fewer parameters, but results are robust to this decision. Because this specification includes the intercept term β_0, which demeans both the observed and predicted trends, the test relies on the spatial pattern of trends around the mean to estimate the climate signal, a characteristic "fingerprint," rather than the absolute magnitude of change. Our statistical test is simply the following: H_0: climate trends have no explanatory power, $\beta_1 = 0$; H_1: climate trends have explanatory power, $\beta_1 > 0$.

This hypothesis is tested using the test statistic $\tau_1 = \hat{\beta_1} \Big/ \sqrt{\widehat{Var}(\hat{\beta_1})}$. In the standard regression model, τ_1 would be normally distributed under the null hypothesis. However, in this case, uncertainty in the response function $f(w)$ means that we cannot rely on the standard normal approximation. Instead, we estimate the distribution of τ_1 under the null using a bootstrap-t procedure that accounts for uncertainty in the parameters of the response function and therefore in the estimation of predicted trends (*Methods*). The 1-α quantile of this distribution then gives us the critical value for a test of size α. We compare τ_1 against the critical value and reject the null if τ_1 is larger, meaning it would be unlikely to occur if the null were true. The value of α is arbitrary, but is conventionally set at 5%, the value we use in this paper.

The second test (test 2) is designed to distinguish a system adapting rapidly from one adapting slowly to climate change impacts. It relies on two regressions:

$$Observed\_Trend_i = \gamma_0 + \gamma_1 Predicted\_Trend\_SR_i + \varepsilon_i, \quad [2]$$

$$Observed\_Trend_i = \gamma_2 + \gamma_3 Predicted\_Trend\_SR_i + \gamma_4 (Predicted\_Trend\_LR_i - Predicted\_Trend\_SR_i) + \varepsilon_i. \quad [3]$$

If farmers have adapted quickly to the climate change experienced, then model 3 should be significantly better at explaining the variance in observed trends than model 2 and therefore should have significantly smaller residuals. We test this with the F statistic $\tau_2 = (RSS_2 - RSS_3)/(RSS_3/(n-3))$, where RSS_2 is the residual sum of squares from model 2 and RSS_3 is the residual sum of squares from model 3. The hypotheses are as follows: H_0: farmers are not adapting, $\tau_2 = 0$; H_1: farmers are adapting, $\tau_2 > 0$.

We use the difference between the long- and short-run predicted trends rather than including them separately in the unrestricted model (model 3) because $Predicted\_Trend\_LR_i$ and $Predicted\_Trend\_SR_i$ are likely to be correlated. Under standard statistical assumptions, τ_2 would have an F distribution, but in this case we again obtain the critical value by imposing the null hypothesis and using a multistage pairs bootstrap to give the distribution of τ_2 under the null (*Methods*).

Before making statistical inferences, it is important to understand the power of the test to detect the signal of interest. If the test has low power, then the probability of a false negative is high and negative results cannot be interpreted either as evidence that climate change has had no impact (test 1) or that there has been no adaptation to climate change (test 2). *SI Appendix*, Table S3 and Figs. S5 and S6 show the results of a simulation analysis designed to determine the power of tests 1 and 2 under a range of reasonable conditions. These results suggest that test 1 should have high power under many conditions. Even if the magnitude of climate trends is small (as is the case in detection and attribution analyses performed today), power can be high if the noise (variation in yield trends from factors not included in the model) is low and variance in the climate trends and baseline climates is large, producing a distinctive signal. For larger climate trends, power is consistently high for most parameter combinations.

In contrast, the simulation suggests that power for test 2 is uniformly very low. Even given large climate trends and large differences in the short- and long-run response curves, power is frequently below 50% and only rarely exceeds 80%. Although arbitrary, the acceptable minimum test power is typically considered to be at least 80%. Thus, in most contexts, reliable statistical detection of climate change adaptation is likely to be challenging. Power may be higher if there is more variable adaptation potential across the landscape (i.e., if the adaptation "fingerprint" is more distinctive) or if specific adaptive changes are being examined. However, in general, these results suggest that studies finding no evidence for adaptation should, in the absence of a power analysis, be interpreted with caution because the probability of false negatives is likely high and a system adapting to climate change cannot be reliably distinguished from one not adapting.

Results

SI Appendix, Fig. S7 shows the simulated power of tests 1 and 2 using the actual climate trends, baseline climate, and noise observed for five European crop yields (*Methods*, *SI Appendix*, Table S4). The short- and long-run response functions were determined statistically using a combination of cross-sectional and interannual variation in yields and growing-season weather (*Methods*, *SI Appendix*, and ref. 8). Consistent with the results of the sensitivity analysis, the power of test 2 is uniformly low. The power of test 1 varies but exceeds 80% for wheat, maize, barley, and sugar beet yields. Power for oilseeds is lower largely because the parameters of the response function are imprecisely estimated (8). This simulation assumes 125 independent data points and therefore, because yields are in reality correlated over space and not independent, gives us an upper bound on test power for our data.

We therefore perform test 1, the detection of climate trend impacts, for wheat, maize, barley, and sugar beet yields. Table 1 shows the results of this statistical test, controlling for linear changes in farm-gate prices and coupled subsidy payments

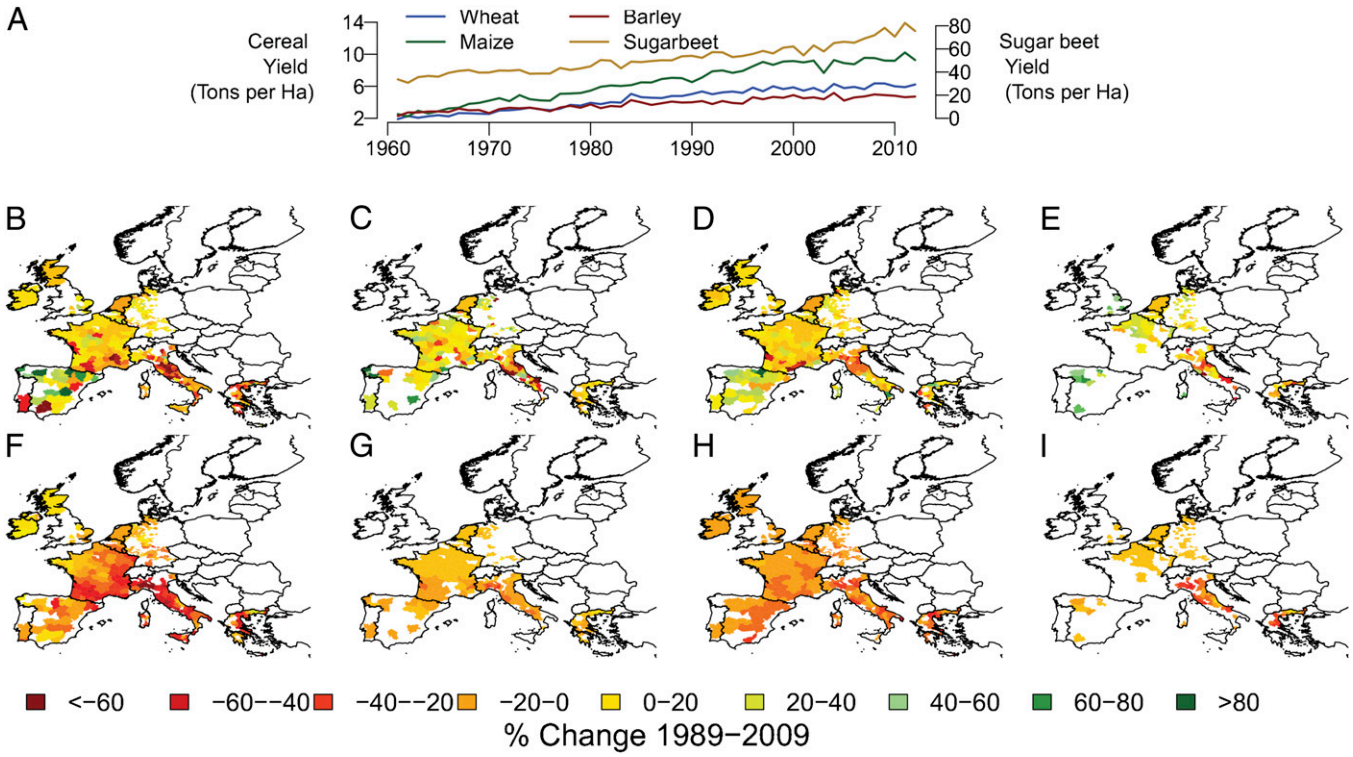

Fig. 1. Patterns and time evolution of crop yields in Europe and the predicted impacts of climate trends. (*A*) Area-weighted yields of the four crops examined in this paper for the countries included in the study, 1960–2010 (*SI Appendix*, Table S1) (17). (*B–E*) Maps of the observed linear trend in yield in 1989–2009 for wheat (*B*), maize (*C*), barley (*D*), and sugar beet (*E*) (25). Maps of the expected change in yield based on growing-season temperature and precipitation trends in 1989–2009 (27, 28) and the yield response functions described by Moore and Lobell (8) (*SI Appendix*, Figs. S3 and S4) for wheat (*F*), maize (*G*), barley (*H*), and sugar beet (*I*). White shows areas not included in the study due to insufficient data.

(*Methods*). We find that the climate change fingerprint is statistically detectable for all crops: the value of the test statistic τ_1 is highly unlikely under the null hypothesis, and thus in all cases we are able to reject, at a test size of 5%, the hypothesis that long-term climate trends have not affected the development of crop yields in Europe. In other words, areas where temperature and precipitation changes realized between 1989 and 2009 would be expected to negatively impact yields have seen yields grow at slower rates compared with areas where climate trends would be expected to have had more positive impacts. The regression coefficients for maize and sugar beet are fairly close to 1, but the wheat and barley coefficients are less than 1, suggesting sensitivity to climate change may be overestimated in the response functions for these crops (15).

SI Appendix, Table S5 gives results for two alternative specifications—one that includes country fixed effects and one that looks only at the impacts of temperature changes, controlling for precipitation change (*Methods*). Adding country fixed effects reduces the risk that results are being driven by unobserved differences in economic or policy conditions between countries (omitted-variable bias). However, because long-term temperature and precipitation trends vary smoothly across space, fixed effects can also remove a large component of the climate signal, exacerbating the effects of measurement error and causing a downward bias on the estimated coefficient (attenuation bias). *SI Appendix*, Table S5 shows that, as expected, country fixed effects reduce the magnitude of the estimated coefficient $\hat{\beta}_1$, although all results are still significant at the 10% level. For wheat yield, adding country fixed effects substantially reduces the magnitude of the regression coefficient, suggesting that this result in particular is driven by intercountry rather than intracountry variation.

Looking at the effect of temperature alone ignores the impact of changing precipitation patterns on yields, but temperature trends are more likely related to anthropogenic climate change than rainfall changes. Although a formal attribution of warming trends to greenhouse gas emissions is outside the scope of this paper, temperature trends tend to be large relative to natural variability and positive across much of Europe (*SI Appendix*, Fig. S1). Power for temperature effects on maize yields is very low so this crop drops out of the analysis, but results for wheat, barley, and sugar beet are consistent with an effect of long-term temperature trends on yields, although the result for wheat is not statistically significant ($P = 0.14$; *SI Appendix*, Table S5).

Discussion

Temperature and precipitation changes in Europe have reduced average production-weighted continent-wide wheat and barley yields by 2.5% and 3.8% and have increased sugar beet and maize yields by 0.2% and 0.3% relative to what they would otherwise be (Fig. 2). These aggregate effects are fairly small, but the impacts have not been evenly distributed. Warmer regions in southern Europe have suffered most from warming, and in Italy this effect has been compounded by drying, leading to yield declines of 5% or more. In cooler regions such as the United Kingdom and Ireland, the more limited impacts of warming have been offset by benefits from increasing rainfall (Fig. 3). These results are consistent with previous work that has found long-term climate trends should have increased sugar beet yields in the United Kingdom, decreased wheat yields in France, and that the yield potential of wheat and barley has declined over much of Europe due to warming (3, 9, 16).

During the 1980s, yields of both wheat and barley were growing at ∼0.12 tons per ha per y (2, 17) (Fig. 1*A*). If they had

Table 1. Results of test 1, the detection of the impact of long-term climate trends on European crop yields

Row name	Wheat yield	Maize yield	Barley yield	Sugar beet yield
Regression coefficient (β_1)	0.41	1.39	0.50	0.82
SE	0.10	0.88	0.34	0.81
Test statistic (τ_1)	4.03	1.58	1.47	1.00
$P(\tau_1 \mid H_0)$	<0.002	0.002	0.012	0.02
Degrees of freedom	349	267	341	183
Adjusted R^2	0.07	0.10	0.06	0.28

The null hypothesis is rejected for all crops at the test size of 5%. Significance levels are determined by a block-bootstrapping procedure that includes resampling the parameters of the climate-yield response function (*Methods*). Although centered on zero, this distribution is skewed to the left, meaning critical values are lower than under standard normality assumptions [critical values for a one-tailed test under the normal approximation are 1.64 (5%) or 1.28 (10%)].

continued growing at that rate after 1995, wheat and barley yields would be 30% and 37% higher today, respectively. This means that climate trends can account for ∼10% of the yield stagnation observed in Europe over the last two decades. Changes in agricultural subsidies and environmental policies, as well as proximity to possible biophysical yield limits, remain likely explanations for the major component of declining yield growth (2, 4, 5). Since 1989, Europe has seen major reforms to its agricultural subsidy policies. Although total support as a fraction of farm revenue has stayed essentially constant, the form of support shifted from price support to direct subsidy payments coupled to production following reforms in 1993, and to decoupled payments not dependent on production after 2004. This means that the fraction of farm support linked to commodity output declined steadily from 87% in 1989 to 27% in 2009 (18) (*SI Appendix*, Fig. S10). This change might be expected to reduce the incentive for intensive cultivation and therefore lower the rate of yield gains. In addition, changing environmental policies restricted the use of fertilizer application and may have limited yield growth (3, 19).

This paper is the first (to our knowledge) to present evidence for the distinctive fingerprint of long-term climate trends on European crop yields and to formally quantify the contribution of a changing climate to yield stagnation in Europe. We find evidence that trends in growing-season temperature and precipitation have affected wheat, maize, barley, and sugar beet yields but estimate that the mean effect across Europe has been relatively small, explaining ∼10% of the slowdown in wheat and barley yield gains since the early 1990s. Impacts have been larger in some regions: the combination of warming and drying trends

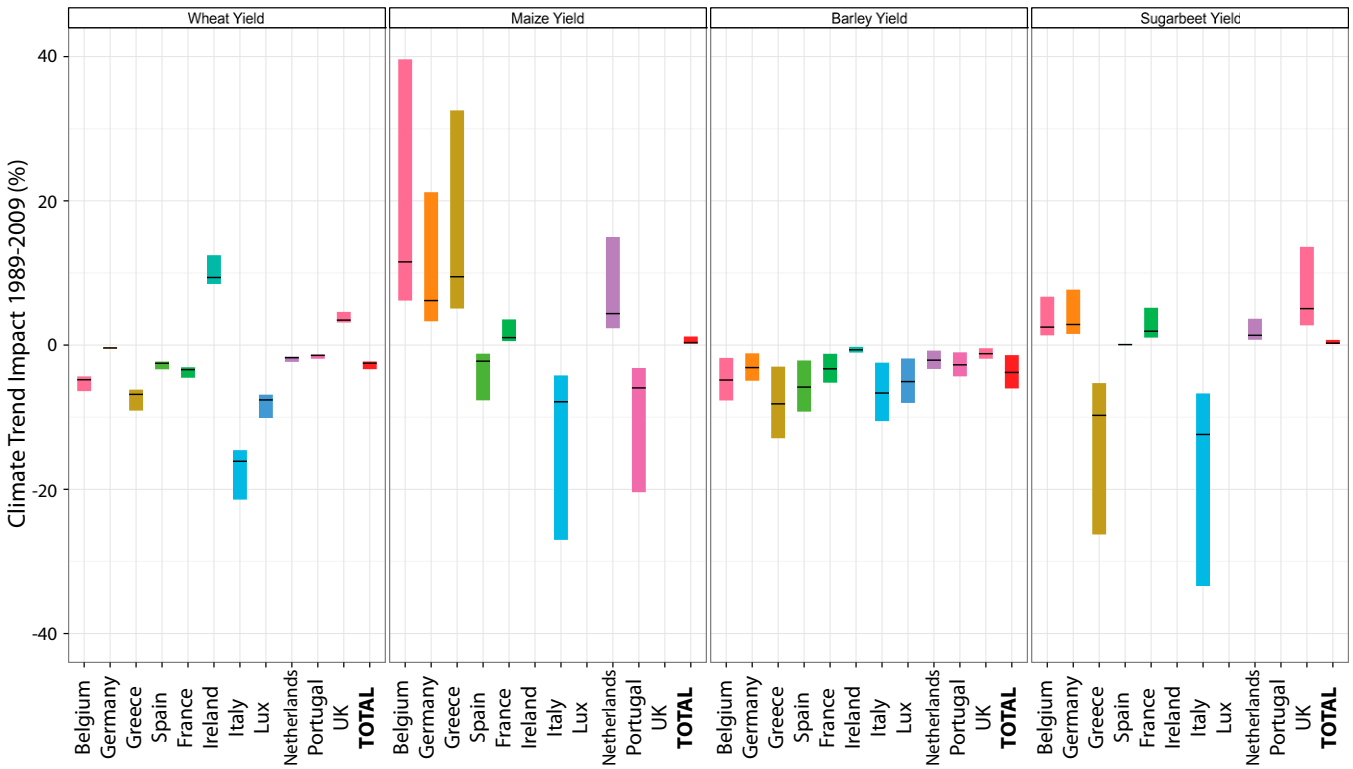

Fig. 2. Impacts of growing-season temperature and precipitation trends in 1989–2009 on European crop yields by country and for the whole region (Total). Impacts are weighted by regional production of the relevant crop in 1989–1994 (*Methods*). The black line shows impacts calculated using the regression point estimate (Table 1), and the colored bars show the 90% confidence interval obtained by inverting a two-tailed hypothesis test of size 10% (*Methods*). This distribution is skewed for wheat, maize, and sugar beet yields, which is why the bars are asymmetric around the point estimate.

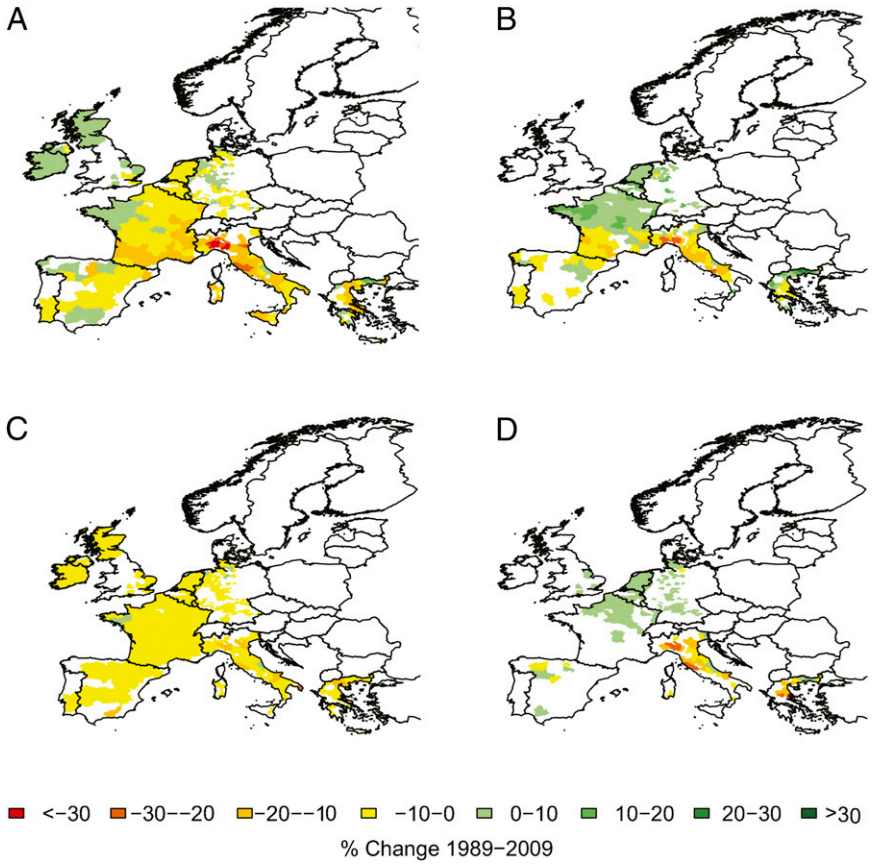

Fig. 3. Spatial fingerprint of trends in growing-season temperature and precipitation in 1989–2009 on wheat (*A*), maize (*B*), barley (*C*), and sugar beet (*D*) yields. The maps show the predicted trends in crop yield due to temperature and precipitation changes (Fig. 1 *F–I*) corrected by the regression coefficient $\widehat{\beta_1}$(Table 1). White shows areas not included in the study due to insufficient data.

in Italy has been particularly damaging, causing yields losses of 10% or more relative to baseline. Although the attribution of European climate trends to greenhouse gas emissions is beyond the scope of this paper, temperature trends are both large relative to natural variability and positive across much of Europe, suggesting they may more likely be linked to anthropogenic climate change than the weaker and more variable precipitation trends (*SI Appendix*, Fig. S1). We estimate that, in the absence of the warming experienced over Europe since 1989, wheat, barley, and sugar beet yields would be 3.5%, 3.8%, and 2.1% higher than they are today (*SI Appendix*, Fig. S9). Finally, this paper presents a formal statistical test for the detection of adaptation to climate change impacts using the difference in projected impacts made including and excluding adaptations. Our simulation analysis shows that the power of this test is likely to be very low in most contexts. Therefore, null results showing no evidence for adaptation to climate change should be interpreted with caution because the probability of false negatives is high, particularly given the relatively small amount of climate change experienced to date.

Methods

Response Function Estimation. All variables were first detrended by fitting linear time trends at the subnational region level. Short- and long-run yield response functions to temperature and precipitation changes were then jointly estimated for each crop using balanced panel data from 1989 to 2009 (8). The long-run response function is a quadratic in both growing-season temperature and rainfall and is estimated using cross-sectional variation in long-term climate, therefore implicitly including substantial adaptation (20). The short-run response function includes an additional penalty term associated with weather that is different from the expected climate and is estimated using interannual variability. It therefore captures the effect of short-term weather variation that is only partly anticipated by farmers and so includes much less adaptation. The preferred model includes controls for soil quality, altitude, irrigation, subsidies, as well as country fixed effects that control for time constant variation between countries (21). Because the long-term linear trends in climate and yield for each region are removed before estimation, they do not influence the response function and therefore ensure the same data are not used to both train the response model and test for the impact of long-run changes in climate. The variance–covariance matrix of response function parameters are estimated using a parametric block-bootstrap at the country level. The estimating equation, response curves, and SEs are given in *SI Appendix*, with additional information in the study by Moore and Lobell (8).

Bootstrap of the Null Distribution. Any detection and attribution study looking at the effect of climate on some outcome of interest (i.e., yields) must account for the fact that the response of that outcome to a given change in climate is uncertain. We account for this additional source of uncertainty by, as part of each bootstrap, creating a new response function by resampling the joint normal distribution of response function parameters and using this to recalculate the predicted trends in yields. Then these new data are resampled, as in a traditional bootstrap, to calculate the distribution of the test statistic under the null (22).

The bootstrap for test 1 uses a version of the bootstrap-t procedure (23). This involves first calculating the regression coefficient $\widehat{\beta_1}$ (Eq. **1**), resampling the parameters of the response function and recalculating predicted trends in yields (to account for uncertainty in the yield response function), resampling the data by country (to account for spatial autocorrelation within countries), and calculating the bootstrapped coefficient $\widehat{\beta_{1\_b}}$. The variance of $\widehat{\beta_{1\_b}}$ is calculated by repeating the previous steps, using the bootstrapped sample, 500 times to give the bootstrapped test statistic $\tau_{1\_b} = (\widehat{\beta_{1\_b}} - \widehat{\beta_1}) \Big/ \left(\sqrt{\widehat{Var}(\widehat{\beta_{1\_b}})}\right)$. Because $\widehat{\beta_1}$ is subtracted in calculating τ_{1_b}, this imposes the null hypothesis (i.e., that τ_{1_b} is equal to zero, in expectation) and so gives the distribution of τ_1 under the null

(22). This procedure is repeated 500 times and the 1-α quantile of the resulting distribution used as the critical value of a one-tailed test of size α. Cameron et al. (23) show that this bootstrap-t procedure improves statistical inference in contexts with clustered data and a small number of clusters relative to the standard cluster-robust errors.

For test 2, each bootstrap is performed by first resampling the parameters of the response function from their joint distribution, recalculating the predicted yield trends using these parameters, and then resampling the data by country. Eq. **2** is then estimated using the bootstrap sample and RSS_{2_b} calculated as the residual sum of squares from that regression. The observed trends are then regressed on the short-run predicted trends and a random variable with the same mean and variance as the difference between the long- and short-run predicted trends and RSS_{3_b} calculated as the residual sum of squares from this regression. The bootstrapped test statistic is calculated as $\tau_{2\_b} = (RSS_{2\_b} - RSS_{3\_b})/(RSS_{3\_b}/(n-3))$. Because the random variable added in the second regression has no true explanatory power, this procedure imposes the null hypothesis in generating the bootstrap and therefore gives the distribution of τ_2 under the null. This procedure is repeated 500 times and the 1-α quantile of the resulting distribution used as the critical value of a test of size α. Step-by-step versions of these procedures are given in *SI Appendix* for clarity.

Estimation of Climate Trend Impacts on Yields. Power for tests 1 and 2 was determined using a simulation exercise parameterized using the European crop and climate data. Data were simulated by creating 125 predicted trends based on the distributions of baseline climates and long-term climate trends in the dataset, and the estimated long- and short-run response functions. White noise was then added with a variance determined by the actual unexplained variance in long-term yield trends in the data to simulate the observed yield trends. Tests 1 and 2 were performed using the simulated data and the bootstrapping procedure described above. This was repeated 500 times to determine the probability of rejecting the null hypothesis for each crop. *SI Appendix*, Table S4 shows the parameter values used for this simulation and additional details on the simulation analysis are given in *SI Appendix*. We also run a simulation to estimate the probability of rejecting a true null hypothesis using test 2 and find this is very close to the desired test size of 5% (*SI Appendix*, Fig. S8).

We conducted tests for which the power exceeds 80% (test 1 for wheat, maize, barley, and sugar beet yields). Linear trends in growing-season temperature and precipitation were estimated for the period 1989–2009 for each region in countries included in the yield response model (*SI Appendix*, Table S1) with at least 10 y of data. The growing season was defined using the observed planting and harvest dates in each region (24). These trends were combined with the baseline climate (1959–1988 mean) and the long-run response function to generate the predicted trends in yields using a local linear approximation of the nonlinear response function:

$$Predicted\_Trend\_Temp_i = \theta_{1,1}(\overline{T}+\Delta T) + \theta_{2,1}(\overline{T}+\Delta T)^2 - \left(\theta_{1,1}\overline{T} + \theta_{2,1}\overline{T}^2\right),$$

$$Predicted\_Trend\_Precip_i = \theta_{1,2}(\overline{P}+\Delta P) + \theta_{2,2}(\overline{P}+\Delta P)^2 - \left(\theta_{1,2}\overline{P} + \theta_{2,2}\overline{P}^2\right),$$

where $\theta_{i,j}$ are the parameters of the long-run response function (*SI Appendix*, Eq. **S1**), $\overline{T}$ and $\overline{P}$ are the baseline growing-season temperature and precipitation climatologies, and ΔT and ΔP are the linear change in growing-season weather between 1989 and 2009.

The observed linear trends in crop yields between 1989 and 2009 are used as the dependent variable. Trends in farm-gate prices between 1989 and 2009 and trends in coupled crop subsidies per hectare of cropland between 1993 and 2009 are included as controls (25). This subsidy control captures the change over this time period from subsidy payments coupled to production to decoupled payments (*SI Appendix*, Fig. S10). The preferred estimating equation is therefore the following:

$$Observed\_Trend_i = \beta_0 + \beta_1(Predicted\_Trend\_Temp_i + Predicted\_Trend\_Precip_i) + \beta_2 Price\_Trend_i + \beta_3 Subsidy\_Trend_i, \quad [4]$$

where the coefficient of interest is β_1, the combined effect of temperature and precipitation changes on yields. *SI Appendix*, Table S5 also presents two alternative specifications, one that includes country fixed effects in Eq. **4** and one that examines only the effect of changing temperature, $Predicted\_Trend\_Temp_i$, including $Predicted\_Trend\_Precip_i$ as a control.

The corrected effect of climate trends on yield in region i is calculated as $\hat{\beta}_1 * (Predicted\_Trend\_Temp_i + Predicted\_Trend\_Precip_i)$ and is shown in Fig. 3. The mean effect in country j is a weighted average:

$$Impact_j = \sum_{i \in j} \hat{\beta}_1 * (Predicted\_Trend\_Temp_i + Predicted\_Trend\_Precip_i) * \frac{P_i}{P_j},$$

where P_i is the mean production in region i over the 5 y at the start of the dataset (1989–1994) and P_j is the same for country j. This assumes that the same climate response ($\hat{\beta}_1$) applies over the whole region because the data available does not allow for a more disaggregated analysis. Ninety percent confidence intervals for the aggregated effect in each country were obtained by inverting the 0.05 and 0.95 quantiles of the bootstrapped distribution of τ_1 to obtain coefficients corresponding to the edges of the rejection region of a two-tailed hypothesis test of size 10% (26).

ACKNOWLEDGMENTS. We thank the Neukermans Family Foundation Stanford Interdisciplinary Graduate Fellowship for funding of this research.

1. Lin M, Huybers P (2012) Reckoning wheat yield trends. *Environ Res Lett* 7:024016.
2. Grassini P, Eskridge KM, Cassman KG (2013) Distinguishing between yield advances and yield plateaus in historical crop production trends. *Nat Commun* 4:2918.
3. Brisson N, et al. (2010) Why are wheat yields stagnating in Europe? A comprehensive data analysis for France. *F Crop Res* 119:201–212.
4. Peltonen-Sainio P, Jauhiainen L, Laurila IP (2009) Cereal yield trends in northern European conditions: Changes in yield potential and its realisation. *F Crop Res* 110:85–90.
5. Finger R (2010) Impacts of agricultural policy reforms on crop yields. *EuroChoices* 7:24–25.
6. Balkhausen O, Banse M, Grethe H (2008) Modelling CAP decoupling in the EU: A comparison of selected simulation models and results. *J Agric Econ* 59(1):57–71.
7. Lobell DB, Schlenker W, Costa-Roberts J (2011) Climate trends and global crop production since 1980. *Science* 333:616–620.
8. Moore FC, Lobell DB (2014) The adaptation potential of European agriculture in response to climate change. *Nat Clim Chang* 4:610–614.
9. Jaggard KW, Qi A, Semenov MA (2007) The impact of climate change on sugarbeet yield in the UK: 1976–2004. *J Agric Sci* 145(4):367–375.
10. Santer BD, et al. (1996) A search for human influence on the thermal structure of the atmosphere. *Nature* 382(6586):39–46.
11. Parmesan C, Yohe G (2003) A globally coherent fingerprint of climate change impacts across natural systems. *Nature* 421(6918):37–42.
12. Cramer W, et al. (2014) *Climate Change 2014: Impacts, Adaptation and Vulnerability. Working Group 2 Contribution to the IPCC 5th Assessment Report* (Cambridge Univ Press, Cambridge, UK).
13. Stone D, et al. (2013) The challenge to detect and attribute effects of climate change on human and natural systems. *Clim Change* 121(2):381–395.
14. Hegerl G, Zwiers F, Tebaldi C (2011) Patterns of change: Whose fingerprint is seen in global warming? *Environ Res Lett* 6:044025.
15. Min SK, Zhang X, Zwiers FW, Hegerl GC (2011) Human contribution to more-intense precipitation extremes. *Nature* 470(7334):378–381.
16. Supit I, et al. (2010) Recent changes in the climatic yield potential of various crops in Europe. *Agric Syst* 103(9):683–694.
17. Food and Agriculture Organization of the United Nations (2014) FAOSTAT, V. 3. Available at faostat.fao.org. Accessed May 2, 2014.
18. Organisation for Economic Co-operation and Development (2013) *Agricultural Policy Monitoring and Evaluation 2013: OECD Countries and Emerging Economies* (Organisation for Economic Co-operation and Development, Paris).
19. Finger R (2010) Evidence of slowing yield growth—the example of Swiss cereal yields. *Food Policy* 35(2):175–182.
20. Mendelsohn R, Nordhaus WD, Shaw D (1994) The impact of global warming on agriculture: A Ricardian analysis. *Am Econ Rev* 84(4):753–771.
21. Van Liedekerke M, Panagos P (2005) *ESDBv2 Raster Archive—a Set of Rasters from the European Soil Database, Version 2.* Available at eusoils.jrc.ec.europa.eu/data.html. Accessed August 22, 2012.
22. MacKinnon JG (2009) *Handbook of Computational Econometrics*, eds Belsley DA, Kontoghiorghes J (Wiley, Chichester, UK), pp 183–213.
23. Cameron AC, Gelbach JB, Miller DL (2008) Bootstrap-based improvements for interence with clustered errors. *Rev Econ Stat* 90(3):414–427.
24. Sacks WJ, Deryng D, Foley JA, Ramankutty N (2010) Crop planting dates: An analysis of global patterns. *Glob Ecol Biogeogr* 19:607–620.
25. European Union (2013) *Farm Accountancy Data Network*. Available at ec.europa.eu/agriculture/rica/. Accessed July 5, 2013.
26. Davidson R, MacKinnon JG (2006) *Palgrave Handbook of Econometrics: Vol. 1, Econometric Theory*, eds Mills TC, Patterson K (Palgrave MacMillan, New York).
27. Matsuura K, Willmott CJ (2009) *Terrestrial Precipitation: 1900–2008 Gridded Monthly Time Series, Version 2.01*. Available at climate.geog.udel.edu/~climate/. Accessed August 13, 2012.
28. Matsuura K, Willmott CJ (2009) *Terrestrial Temperature: 1900–2008 Gridded Monthly Time Series, Version 2.01*. Available at climate.geog.udel.edu/~climate/. Accessed August 13, 2012.

The Fingerprint of Climate Trends on European Crop Yields: Supplementary Information Appendix

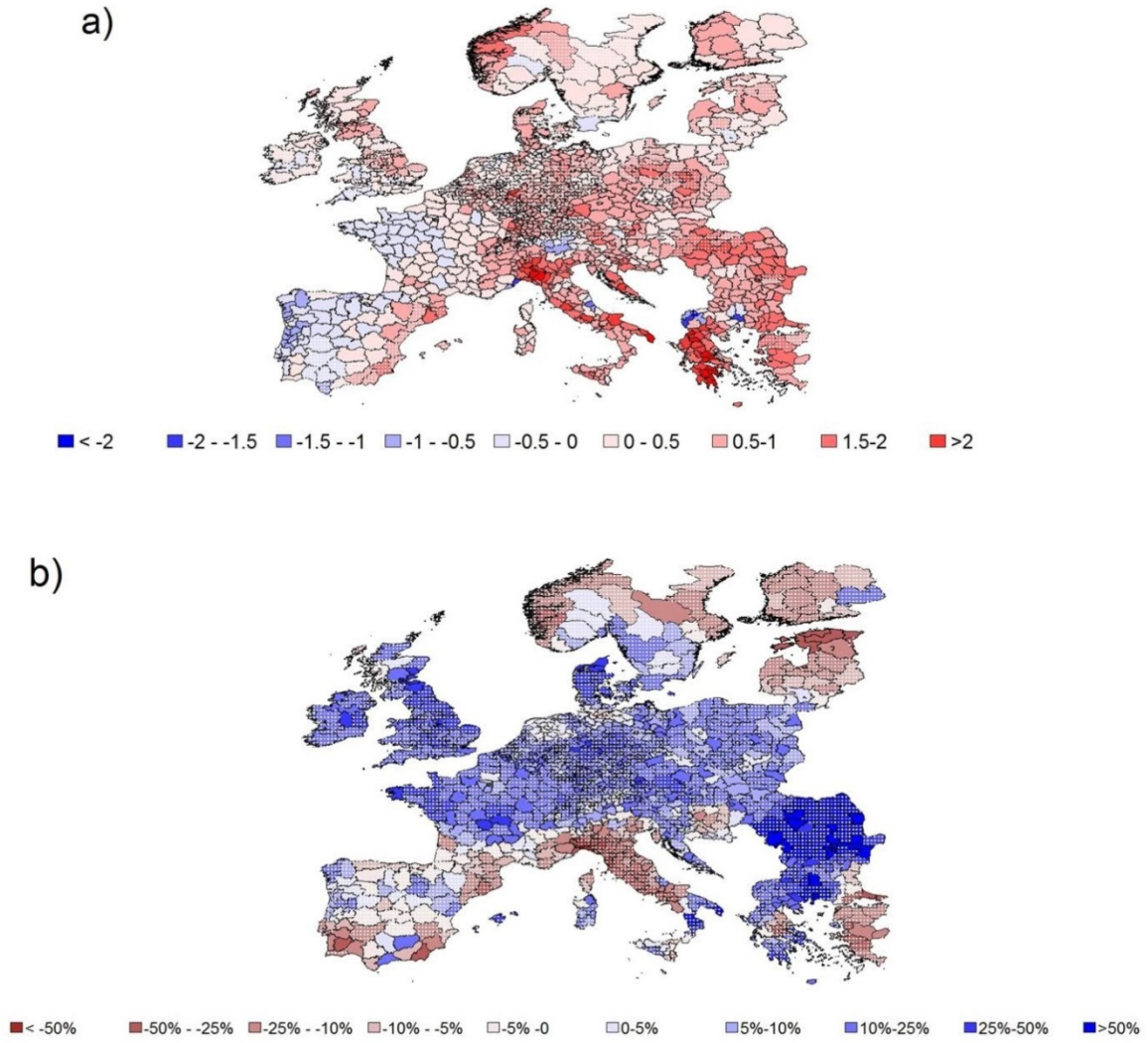

Figure S1: March – September temperature (°C) and precipitation (mm per month) changes over Europe based on linear time trends 1989-2009(1, 2). White stippling shows regions where the long-term trend is not statistically significant at the 10% level.

Crop	Countries Included
Wheat	Belgium, France, Germany, Greece, Ireland, Italy, Luxembourg, Netherlands, Portugal, Spain, UK.
Maize	Belgium, France, Germany, Greece, Italy, Netherlands, Portugal, Spain.
Barley	Belgium, France, Germany, Greece, Ireland, Italy, Luxembourg, Netherlands, Portugal, Spain, UK.
Sugarbeet	Belgium, France, Germany, Greece, Italy, Netherlands, Spain, UK.

Table S1: Countries with regions included in this study. The spatial extent of the study is limited by the need for a sufficient length of data from which to calculate a reliable estimate of the long-term yield trend (set at 10 years) and the limited generalizability of the yield-response model. For these reasons, eastern Europe is not included in the analysis.

Supplementary Methods

1. Estimation of Long- and Short-Run Response Curves
2. Bootstrap of the Null Distribution
3. Power Simulation Analysis

1. Estimation of Long- and Short-Run Response Curves

The short- and long-run responses of yield to temperature and precipitation changes are jointly estimated using panel data. Our source of economic and yield data is the EU Farm Accountancy Data Network (FADN) survey between 1989 and 2009, aggregated from the farm to the regional (sub-national) level (3). Yields are calculated as the crop produced in the year divided by the area of crop planted. Weather and climate data are monthly means averaged over the growing season defined using the observed planting and harvest dates for each region (for winter crops, the 4 months prior to the observed harvest date) (1, 2, 4).

The yields across Europe are modelled as a quadratic in average growing-season temperature and average growing-season precipitation using the same response function across the region. All time-trending variables are first de-trended using linear time-trends for each sub-national region. This step removes all long-term trends (the source of variation used for Tests 1 and 2 presented in this paper) and thus avoids any risk that the same data is being used to both train the response model and test for evidence of climate trend impacts.

De-trended log yields (Y) for sub-national region i, in country j in year t are estimated as:

$$Y_{ijt} = \theta_0 + \boldsymbol{\theta_1}\overline{W}_{ij} + \boldsymbol{\theta_2}\overline{W}_{ij}^2 + \boldsymbol{\theta_3}(W_{ijt} - \overline{W}_{ij})^2 + \theta_{4,j}Country_j + \boldsymbol{\theta_5}Controls_{ijt} + \varepsilon_{ijt} \qquad (Eq\ S1)$$

where W_{ijt} is a vector that includes growing season temperature and precipitation and $\overline{W}_{ij}$ is the 30-year climatological average over the baseline period (1958-1988). Bold denotes vectors of coefficients. Our de-trending step removes the effect of unobserved time-trends at the sub-national region level. We control for unobserved time-constant variation between countries using a country fixed effect and other observed within-country variation using a suite of controls. These include a vector of soil-quality variables (organic carbon content, water-holding capacity, erodibility, and soil type), altitude and altitude squared, subsidies received per Ha, and irrigated area per Ha (5). This equation is estimated using OLS regression, weighting by the square root of crop area to reduce heteroskedasticity and to make results more representative of the average growing area. This method uses cross-sectional variation in baseline climate to estimate the long-run response of yields to changing climate and inter-temporal deviations in growing-season weather from baseline climate to estimate the short-run impact of weather shocks. It is very similar to the method described in Moore and Lobell (6), but with the added initial step of de-trending at the sub-national level. This results in nearly identical coefficients but explicitly removes any concerns of training and testing on the same data.

Given a change in climate in region i from $\overline{W}_{0i}$ to $\overline{W}_{1i}$, the long-run response $\left(\Delta\hat{Y}_{LR}\right)$is defined as:

$$\Delta\hat{Y}_{LRi} = \widehat{\boldsymbol{\theta_1}}(\overline{W}_{1i} - \overline{W}_{0i}) + \widehat{\boldsymbol{\theta_2}}\left(\overline{W}_{1i}^2 - \overline{W}_{0i}^2\right)$$

Because the parameters of this response function are estimated using cross-sectional variation in the 30-year mean baseline climate, this relationship between climate and yields implicitly includes all adaptations used by farmers within the region. This is under the assumption that farmers have fully adjusted to their baseline climate and that the relative prices of crops and inputs has remained constant (7). The short-run response ($\Delta\hat{Y}_{SR}$) is defined as:

$$\Delta\hat{Y}_{SRi} = \widehat{\boldsymbol{\theta_1}}(\overline{W}_{1i} - \overline{W}_{0i}) + \widehat{\boldsymbol{\theta_2}}\left(\overline{W}_{1i}^2 - \overline{W}_{0i}^2\right) + \widehat{\boldsymbol{\theta_3}}(\overline{W}_{1i} - \overline{W}_{0i})^2$$

This is the same as $\Delta\hat{Y}_{LR}$ but includes the additional term $\widehat{\boldsymbol{\theta_3}}(\overline{W}_{1i} - \overline{W}_{0i})^2$, which can be interpreted as a penalty associated with being imperfectly adjusted to the new climate, $\overline{W}_{1i}$, which is different from the expected baseline climate, $\overline{W}_{0i}$ (since the estimated $\widehat{\boldsymbol{\theta_3}}$ is negative). This penalty term is estimated using inter-annual weather fluctuations ($W_{ijt} - \overline{W}_{ijt}$) in the panel data-set (Eq S1). Since these weather fluctuations are transient and at least partly unanticipated, farmers have a more limited set of adjustments than are employed in response to long-term climatic differences. Figure S2 gives a diagrammatic representation of these short- and long-term response curves under the parametric assumptions of the estimating equation.

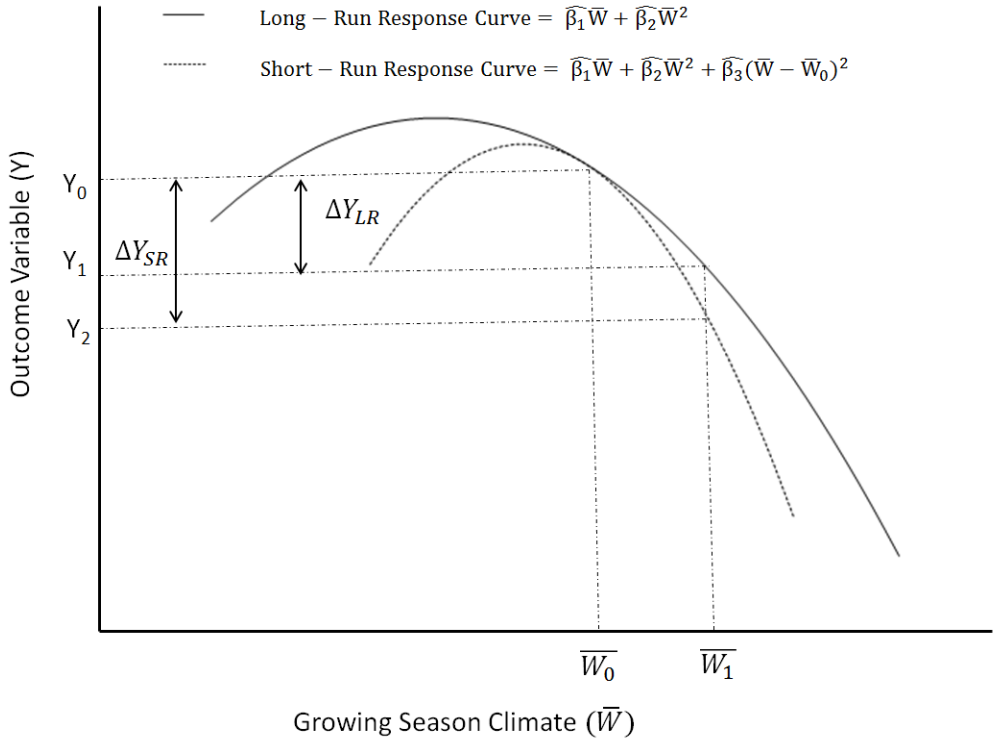

Figure S2: Diagrammatic representation of short- and long-run responses to a shift in climate from $\overline{W}_0$to $\overline{W}_1$ given the functional-form assumptions of the estimating equation (Equation S1).

Figures S3 and S4 show the temperature and precipitation response curves used in this paper. Standard errors for the parameters of these response curves are estimated using 500 block-bootstraps, blocking at the country by two-year level to account for heteroskedasticity, within-country spatial autocorrelation, and temporal autocorrelation at one-year lag and are given in Table S2. A fuller description of this estimation procedure, robustness checks, and standard errors can be found in Moore & Lobell (6).

	Wheat Yield	Maize Yield	Barley Yield	Sugarbeet Yield
	(1)	(1)	(1)	(1)
Mean Temp	0.1552 *	0.0137	0.1655 ***	0.3482 ***
	0.078	0.020	0.0433	0.068
Mean Temp^2	-0.017 ***	0.0000	-0.012 ***	-0.011 ***
	0.003	0.0006	0.002	0.002
(Temp-Mean Temp)^2	-0.0181 *	-0.0299 ***	-0.0287 ***	-0.0252 ***
	0.0073	0.0086	0.006	0.004
Mean Precip	0.0168 ***	0.0085 ***	0.001	0.0032 **
	0.0022	0.001	0.0021	0.001
Mean Precip^2	-5.09E-05 ***	-3.18E-05 ***	-8.73E-06	-6.16E-06
	8.78E-06	4.56E-06	7.80E-06	4.47E-06
(Precip-Mean Precip)^2	-2.35E-05	-2.02E-05 ·	-2.46E-05 ·	-8.60E-06
	1.69E-05	1.11E-05	1.30E-05	1.20E-05

· p<0.1; *p<0.05; **p<0.01;***p<0.001

Table S2: Response function coefficients for the response model shown in Equation S1 and standard errors based on 500 block-bootstraps with blocks defined at the country by two-year level to account for heteroskedasticity, spatial autocorrelation and temporal autocorrelation with one year lag.

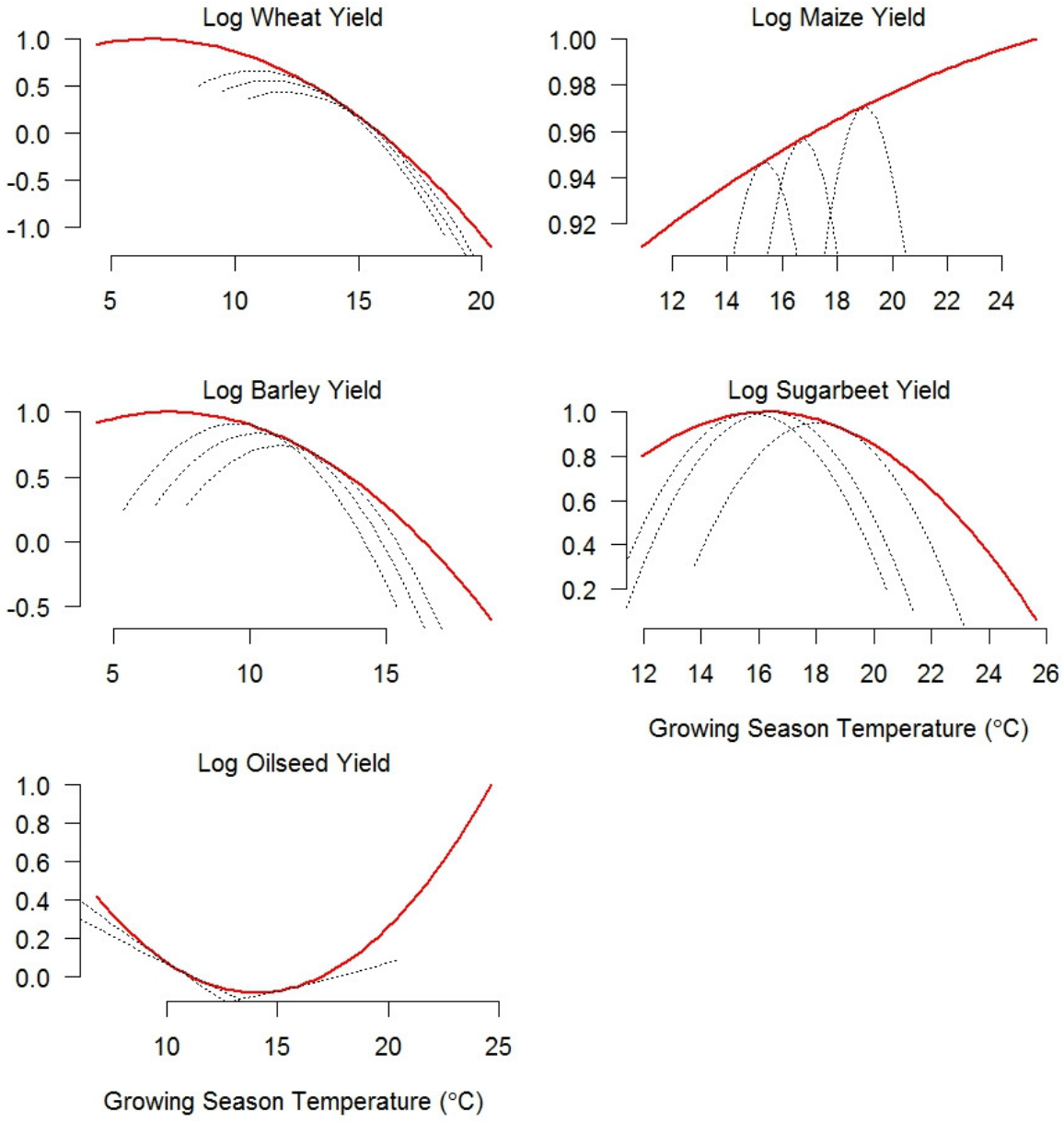

Figure S3: Graphical depiction of the long-run (red solid line) and short-run (black dotted line) relationship between de-trended yields and de-trended growing season temperature estimated using Equation S1. The range of the x-axis corresponds to the range of growing season temperature in each panel dataset. The three examples of short-run relationships are plotted centered at the 25th, 50th, and 75th percentiles of growing-season temperature. Curves are shifted along the y-axis so that the maximum value over the plotting range is 1. Because the dependent variable is logged, movement along the y-axis represents a % change in the outcome variable.

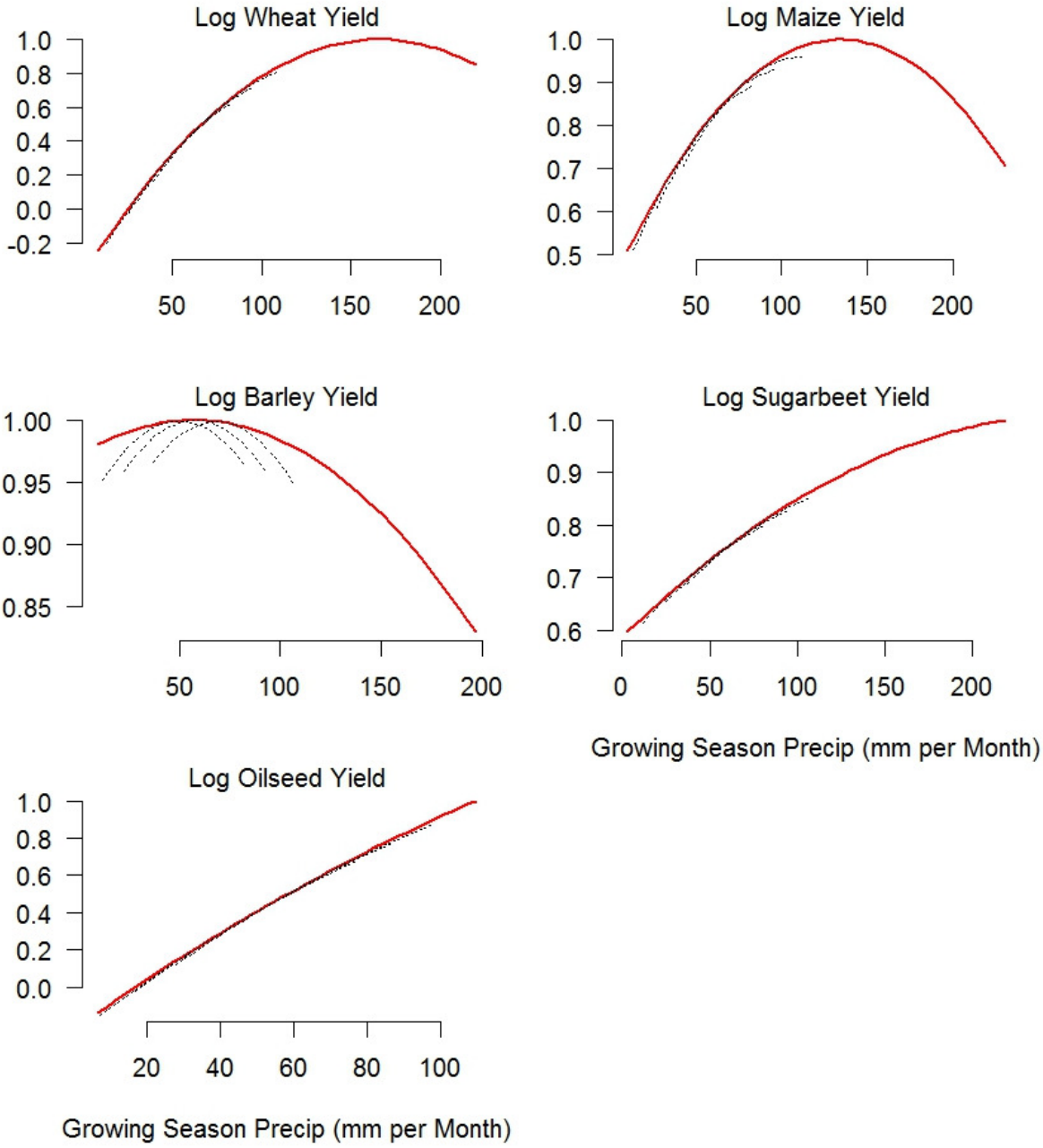

Figure S4: Graphical depiction of the long-run (red solid line) and short-run (black dotted line) relationship between de-trended yields and de-trended growing season precipitation estimated using Equation S1. The range of the x-axis corresponds to the range of growing season precipitation in each panel dataset. The three examples of short-run relationships are plotted centered at the 25th, 50th, and 75th percentiles of growing-season precipitation. In many cases the short-run response curves are not visible because they overlie the long-run response curves. Curves are shifted along the y-axis so that the maximum value over the plotting range is 1. Because the dependent variable is logged, movement along the y-axis represents a % change in the outcome variable.

2. Bootstrap of the Null Distribution

The procedures used to estimate the distribution of the test statistics under the null hypotheses are described in the Methods section, but a step-by-step procedure is provided here for additional clarity. For both tests, the procedure accounts for uncertainty in the estimation of the yield response function by resampling the parameters of the response function from their joint multivariate normal distribution estimated using the block-bootstrap described in the previous section.

Test 1

1. Estimate the regression shown in Equation 1 (Main Text) to give the coefficient estimate $\hat{\beta}_1$
2. Estimate $Var(\hat{\beta}_1)$:
    i. Resample the parameters of the response function ($\boldsymbol{\theta_{1\_b}}$ and $\boldsymbol{\theta_{2\_b}}$) from their joint distribution
    ii. Recalculate predicted yield trends using these parameters
    iii. Resample the data by country
    iv. Recalculate $\hat{\beta}$
    v. Repeat 2.i to 2.iv 500 times and take the variance of these estimates
3. Calculate the test statistic $\tau_1 = \frac{\widehat{\beta_1}}{\sqrt{\widehat{Var}(\widehat{\beta}_1)}}$
4. Resample the parameters of the response function
5. Recalculate predicted yield trends using these parameters
6. Resample the data by country
7. Calculate the bootstrapped estimate $\hat{\beta}_{1\_b}$
8. Estimate $Var(\hat{\beta}_{1\_b})$ by repeating steps 2.i – 2.v using the bootstrapped sample
9. Calculate the bootstrapped test statistic, imposing the null hypothesis $\tau_{1\_b} = \frac{\widehat{\beta}_{1\_b} - \widehat{\beta_1}}{\sqrt{\widehat{Var}(\widehat{\beta}_1)}}$
10. Repeat 4-9 500 times
11. Fine the 95th quantile of the distribution to give the critical value for the (one-sided) test of size 5%.

This is a version of bootstrap-t procedure using a double-bootstrap described by both MacKinnon (8) and Cameron, Gelbach and Miller (9). Block-bootstrapping by country accounts for both heteroskedasticity and correlation of the error terms within countries while directly bootstrapping the t-statistic provides improved inference in cases with relatively few clusters (countries), as is the case here (9). Resampling the parameters of the response function and recalculating the predicted trends accounts for the fact that the climate-yield response function is not known exactly.

Test 2

1. Estimate Equations 2 and 3 (Main Text) and calculate $\tau_2 = \frac{RSS_2 - RSS_3}{RSS_3/(n-3)}$

2. Resample the parameters of the response function ($\boldsymbol{\theta_{1\_b}}$ and $\boldsymbol{\theta_{2\_b}}$) from the joint distribution
3. Recalculate predicted yield trends using these parameters
4. Resample the data by country
5. Calculate the bootstrapped estimate τ_{2_b}, imposing the null hypothesis:
    i. Calculate RSS_{2_b} from the resampled data
    ii. Calculate the mean and variance of the difference between the long-run and short-run predicted trends in the resampled data
    iii. From the resampled data, regress the observed trends on the short-run predicted trends and a random variable with the same mean and variance calculated in 5.ii
    iv. Use the residuals from this regression to calculate RSS_{3_b}
    v. $\tau_{2\_b} = \frac{RSS_{2\_b} - RSS_{3\_b}}{RSS_{3\_b}/(n-3)}$
6. Repeat 2-5 500 times
7. Find the 95th quantile of the distribution to give the critical value for a (one-tailed) test of size 5%.

This procedure both accounts for uncertainty in the response function through the resampling of parameters, and potential heteroskedasticity and spatial autocorrelation. The bootstrapping procedure imposes the null hypothesis (that the additional variable in the second, unrestricted regression has no explanatory power) by adding a random variable rather than the true variable, therefore giving the sampling variability of τ_2 under the null hypothesis.

3. Power Simulation Analysis

The goal of the power simulation analysis was to determine under what conditions Test 1 and Test 2 might be expected to have sufficient power (>80%) for reliable inference. Because of computational limitations, a single long-run response function was used (the sugarbeet temperature response function, Table S2). This gives a moderately sensitive, non-linear response to warming over the region of interest (Fig S3) and therefore might be expected to give higher power compared to flatter or more linear response functions. For each parameter that might affect statistical power, a high and low value were determined based on realistic values informed by the European dataset. Additional levels of noise were included because of the importance of this parameter. These parameters were combined in a full factorial design for the power simulation.

Parameter	Fixed Value	V. Low Value	Low Value	Mid Value	High Value
Magnitude Climate Trend	--	--	0.5°C	--	5°C
Variance Climate Trend	--	--	$0.5°C^2$		$2°C^2$
Theta1	$0.348°C^{-1}$	--	--	--	--
Theta2	$-0.011°C^{-2}$	--	--	--	--
Theta3	--	--	$-0.005°C^{-1}$	--	$-0.03°C^{-1}$
Variance Baseline Climate	--	--	$2°C^2$	--	$6°C^2$
Noise Variance	--	0.05	0.5	1	5
Response Function Uncertainty	$\begin{bmatrix} 4.56*10^{-3} & -1.40*10^{-4} \\ -1.40*10^{-4} & 4.32*10^{-6} \end{bmatrix}$	--	--	--	--
Sample Size	125	--	--	--	--
Test Size	5%	--	--	--	--

Table S3: Parameter values used in the power simulation analysis. These were combined in a full factorial design and power was calculated using 200 simulations for each combination of parameters. The response function parameters (Theta1 and Theta2) and their variances were taken from the sugarbeet temperature response function (Figure S3).

Each simulation involved drawing a sample of 125 hypothetical baseline climates and climate trends from two independent normal distributions defined by the parameters in Table S3 (the mean of the baseline climates was fixed at 17°C, the optimum of the sugarbeet yield response curve). Yield trends were predicted with and without adaptation using the long- and short-run yield response functions respectively. Then "observed" yield trends were generated by adding white noise (with a variance defined in Table S3) to the predicted long-run trends, representing the variation in yield trends not explained by climate trends or other control variables. Tests 1 and 2 were then performed, with the distribution of the test statistics under the null estimated using the simulated data as described in Methods and the SI. This was repeated 200 times for each combination of parameter values to determine the probability of rejecting the null hypothesis, equivalent to the power of the test since the alternative hypothesis is true in the simulations by construction. Results are given in Figure S5 (Test 1) and Figure S6 (Test 2).

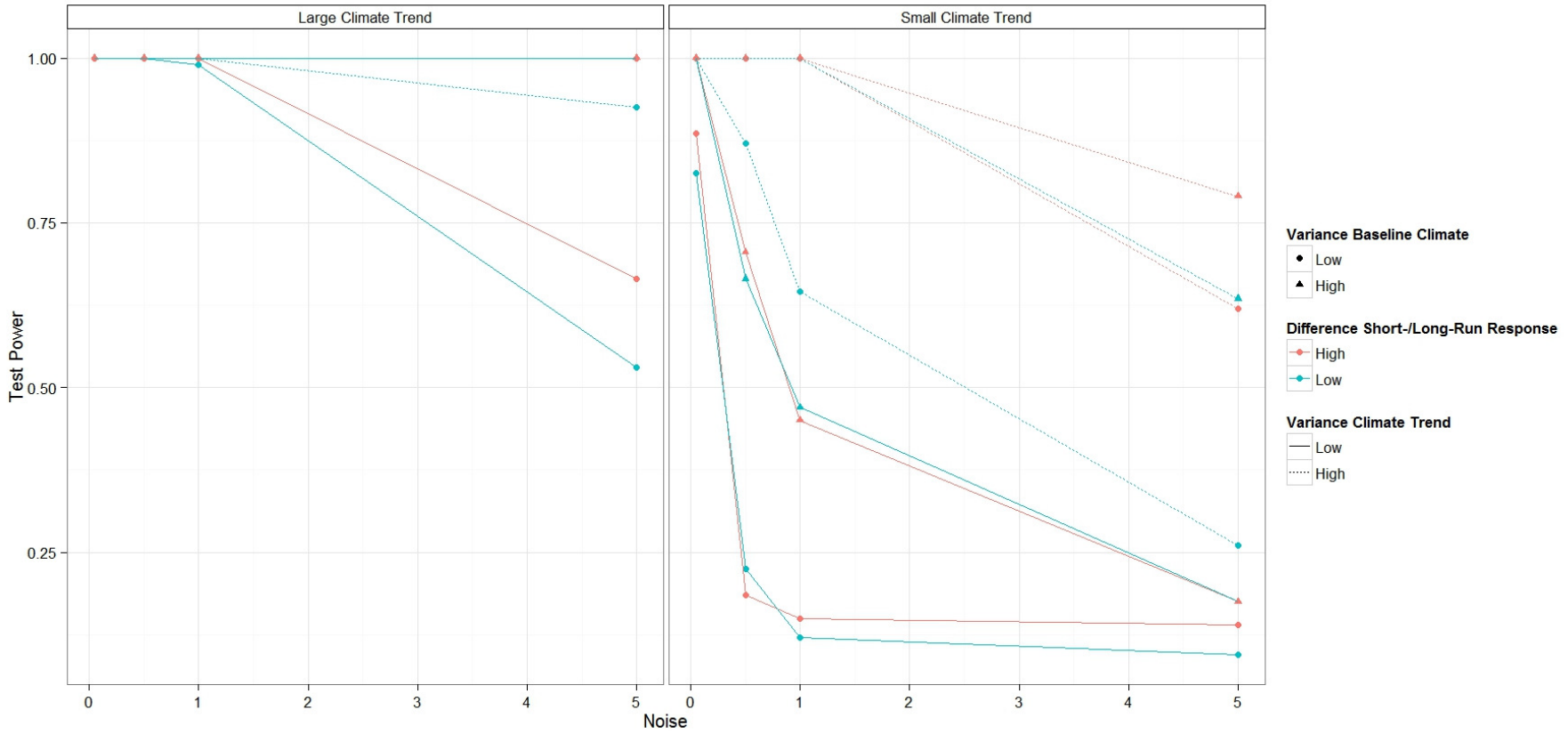

Figure S5: Simulated power (probability of rejecting the null hypothesis, conditional on the alternative being true) of Test 1 (detection of climate change impacts) under various parameter combinations. Power is consistently high when the climate trend is large (5°C) and can be high even if the climate trend is small (0.5°C) in certain contexts. Power is based on 200 simulations for each combination of parameter values and inference is made using 200 bootstraps for each simulation. Parameter values used for the simulation are shown in Table S3.

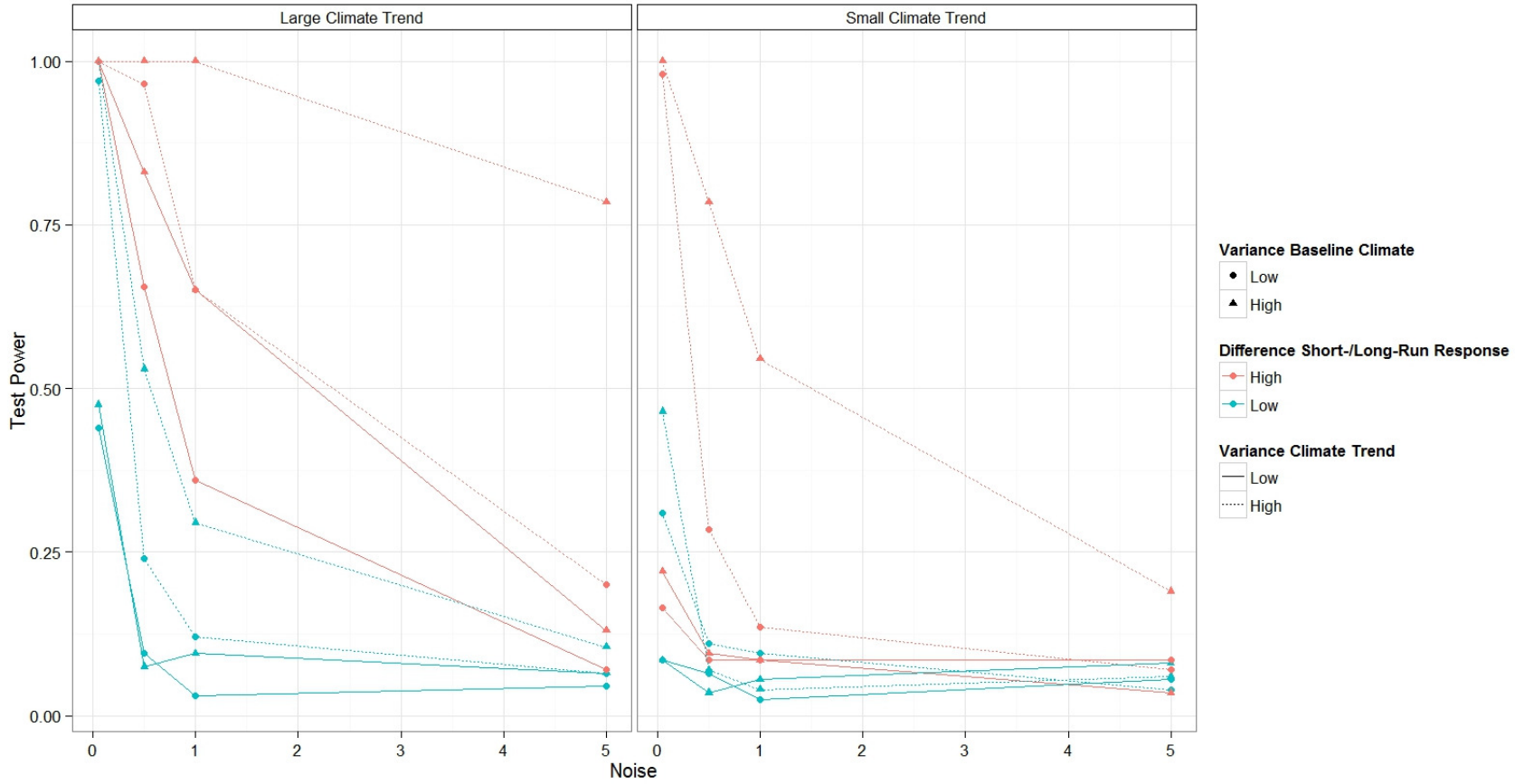

Figure S6: Simulated power (probability of rejecting the null hypothesis, conditional on the alternative being true) of Test 2 (detection of climate change adaptation) under various parameter combinations. Power is consistently low, even when the climate trend is large. Power is based on 200 simulations for each combination of parameter values and inference is made using 200 bootstraps for each simulation. Parameter values used for the simulation are shown in Table S3.

Parameter	Units	Log Wheat Yield	Log Maize Yield	Log Barley Yield	Log Sugarbeet Yield	Log Oilseed Yield
Mean Temperature Trend	°C per 20 years	0.97	0.77	0.75	0.68	0.60
Variance Temperature Trend	(°C per 20 years)^2	0.24	0.51	0.20	0.37	0.16
Mean Precipitation Trend	mm per Month per 20 years	4.4	-2.1	4.6	4.0	8.4
Variance Precipitation Trend	(mm per Month per 20 years)^2	198	289	143	320	104
Variance Baseline Temperature	°C^2	2.8	5.4	3.6	6.6	13.7
Variance Baseline Precipitation	(mm per Month)^2	554	904	458	737	161
Noise Variance	(% per 20 Years)^2	8.2	13.1	5.0	5.8	19.6

Table S4: Parameters used to estimate power of Tests 1 and 2 for 5 European crops. Temperature and precipitation values are calculated for the crop- and region-specific growing seasons defined using observed planting and harvest dates(4). Noise was calculated based on the variance of residuals from a regression of the observed trend on all explanatory variables (predicted climate trend, trend in coupled subsidies, and trend in prices).

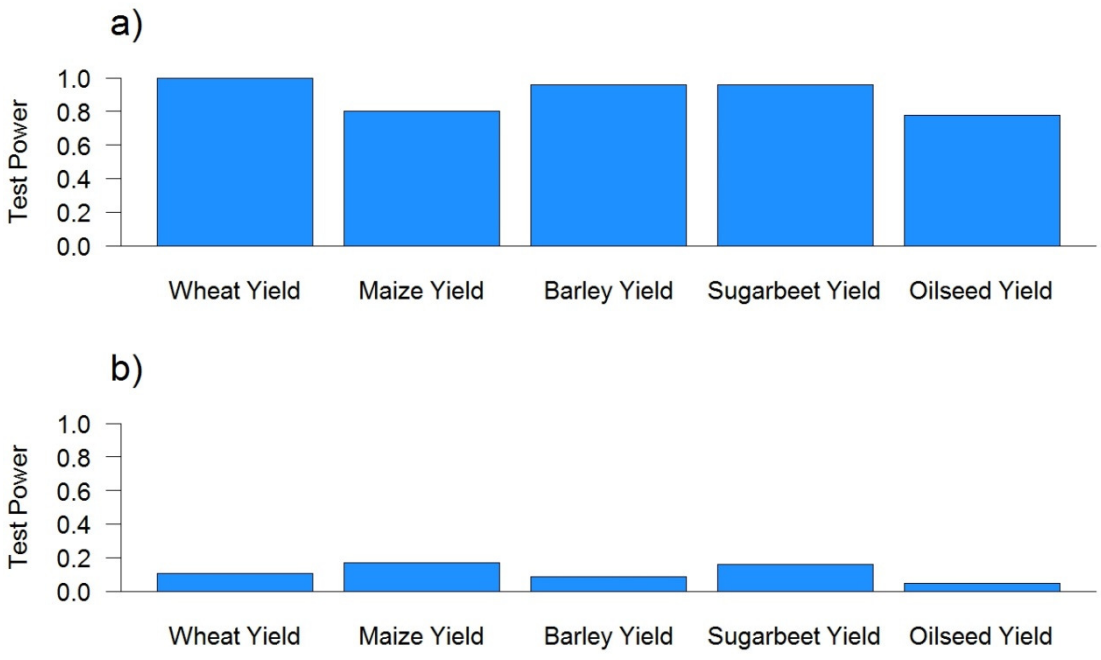

Figure S7: Estimated power of statistical tests for a) the detection of climate change impacts (Test 1) and b) the detection of adaptation to those impacts (Test 2) for observed values of climate trends, response functions, and baseline climate for 5 crops in Europe (Table S4). Power is estimated using 500 simulations for each crop and, for each simulation, inference is made using 500 bootstraps. Each simulation uses 125 independent data points, which may overestimate the number of independent data points in our dataset because of spatial autocorrelation. These should therefore be considered upper bounds for the true power of these tests for this dataset.

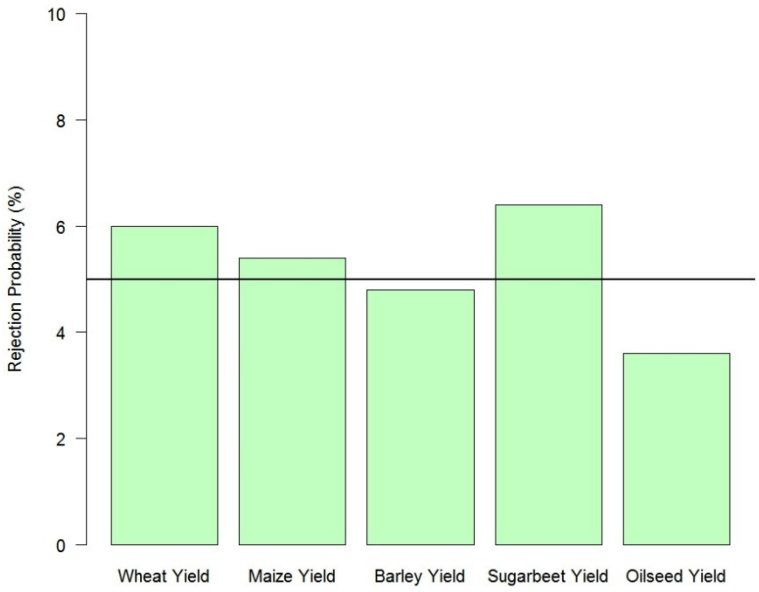

Figure S8: Probability of rejecting a true null hypothesis for Test 2 (the detection of climate change adaptation) estimated using 500 simulations for all crop yield response curves. The horizontal black line shows the desired test size of 5%. Rejection probabilities are close to 5% for all crops, though the test may be slightly conservative for oilseed yields.

Supplementary Results

Panel A	Wheat Yield		
	(1)	(2)	(3)
Regression Coefficient (Beta1)	0.41	0.07	0.22
Standard Error	0.10	0.12	0.29
Test Statistic (Tau1)	4.03	0.57	0.77
P(Tau1|H0)	<0.002	0.06	0.14
Degrees of Freedom	349	339	348
Adjusted R2	0.07	0.20	0.08

Panel B	Maize Yield		
	(1)	(2)	(3)
Regression Coefficient (Beta1)	1.39	0.30	--
Standard Error	0.88	0.24	--
Test Statistic (Tau1)	1.58	1.23	--
P(Tau1|H0)	0.002	0.02	--
Degrees of Freedom	267	260	--
Adjusted R2	0.1	0.22	--

Panel C	Barley Yield		
	(1)	(2)	(3)
Regression Coefficient (Beta1)	0.50	0.39	0.50
Standard Error	0.34	0.43	0.32
Test Statistic (Tau1)	1.47	0.91	1.24
P(Tau1|H0)	0.012	0.02	0.01
Degrees of Freedom	341	331	340
Adjusted R2	0.06	0.11	0.04

Panel D	Sugarbeet Yield		
	(1)	(2)	(3)
Regression Coefficient (Beta1)	0.82	0.31	1.31
Standard Error	0.81	0.48	0.38
Test Statistic (Tau1)	1.00	0.65	2.31
P(Tau1|H0)	0.02	0.06	0.01
Degrees of Freedom	183	176	182
Adjusted R2	0.28	0.43	0.30

Table S5: Results of Test 1 for the preferred model (1) and alternative specifications. (2) includes country fixed-effects in Equation 4 (Methods) and (3) shows the effect only of temperature changes, with precipitation changes included as a control (Methods). Because of the limited sensitivity of maize yields to temperature in this region (Figure S3), power for maize yields is much lower than 80% and so specification (3) was not conducted.

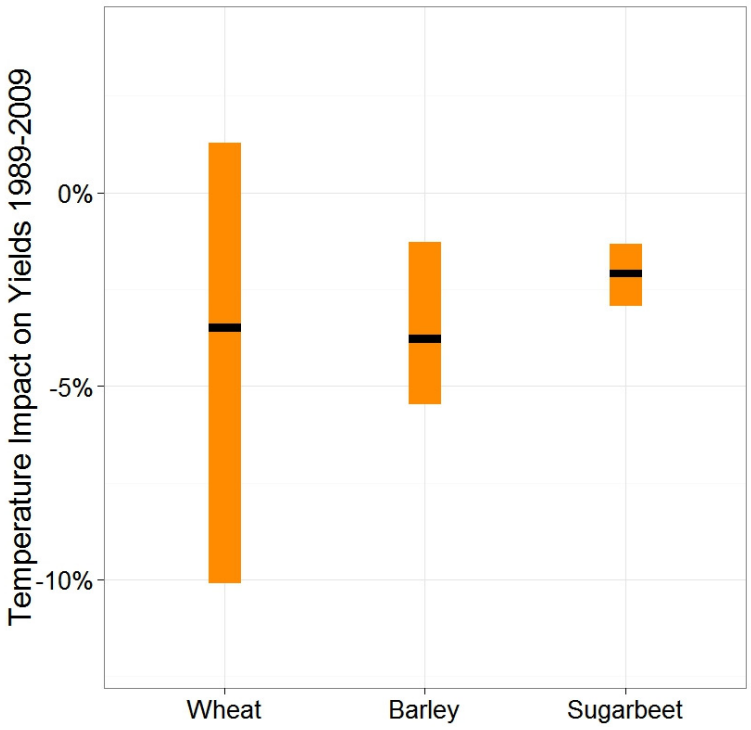

Figure S9: Mean impact of growing-season temperature trends 1989-2009 on wheat, barley, and sugarbeet yields based on the predicted yield trends due to temperature changes and the estimated coefficient shown in Table S5, column 3. The black line shows the point estimate and the orange bar shows the 90% confidence interval obtained by inverting a two-tailed hypothesis test of size 10% (Methods). Impacts are weighted by regional production of the relevant crop 1989-1994 (Methods).

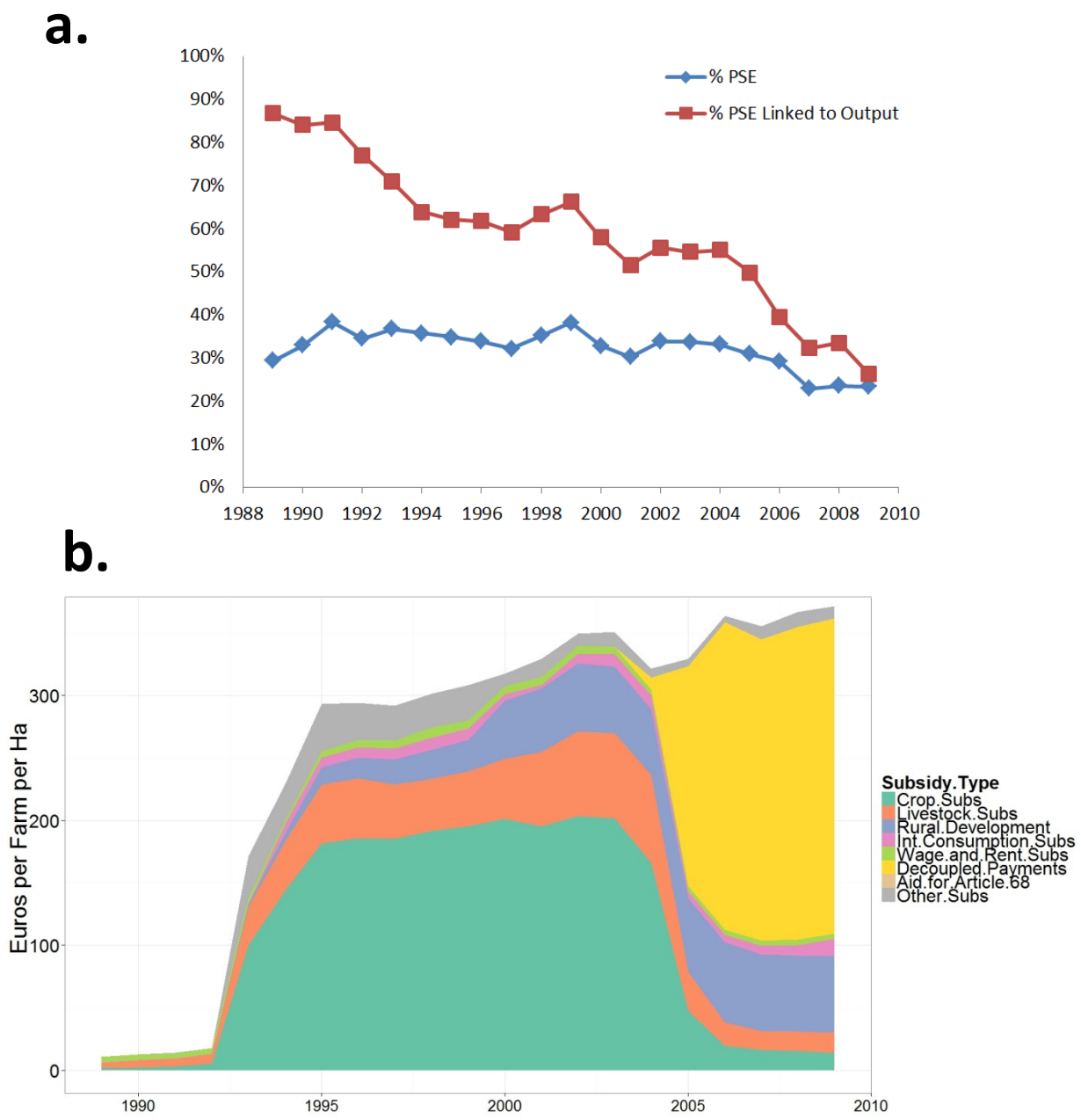

Figure S10: Changes in the form of European farm support. a) Producer Support Equivalent (PSE) in the EU-15, a measure of total taxpayer support to farmers through both price support and subsidy payments. The graph shows both total support as a percentage of farm revenues (%PSE) and the percent of total support linked to commodity production (% PSE Linked to Output) as either price support or payments coupled to production (10). b) Changes in the form of EU subsidy payments. Prior to 1993, agricultural support took the form of direct price supports, not shown in this graph. Between 1993 and 2005, farmers received payments coupled to crop and livestock production (Crop Subsidies and Livestock Subsidies). After 2005, subsidy payments were not based on production but simply on farm size and type (Decoupled Payments) (3).

References

1. Matsuura K, Willmott CJ (2009) Terrestrial Precipitation: 1900-2008 Gridded Monthly Time Series Version 2.01. Available at: http://climate.geog.udel.edu/~climate/.

2. Matsuura K, Willmott (2009) Terrestrial Temperature: 1900-2008 Gridded Monthly Time Series Version 2.01. Available at: http://climate.geog.udel.edu/~climate/.

3. EU (2013) Farm Accountancy Data Network. Available at: ec.europa.au/agriculture/rica/index.cfm [Accessed July 5, 2013].

4. Sacks WJ, Deryng D, Foley JA, Ramankutty N (2010) Crop Planting Dates: An Analysis of Global Patterns. *Glob Ecol Biogeogr* 19:607–620.

5. Van Liedekerke M, Panagos P (2005) *ESDBv2 Raster Archive - a Set of Rasters from the European Soil Database Version 2* Available at: http://eusoils.jrc.ec.europa.eu/data.html.

6. Moore FC, Lobell DB (2014) The Adaptation Potential of European Agriculture in Response to Climate Change. *Nat Clim Chang* 4:610–614.

7. Mendelsohn R, Nordhaus WD, Shaw D (1994) The Impact of Global Warming on Agriculture: A Ricardian Analysis. *Am Econ Rev* 84:753–771.

8. MacKinnon JG (2009) in *Handbook of Computational Econometrics*, eds Belsley DA, Kontoghiorghes J (Wiley, Chichester), pp 183–213.

9. Cameron AC, Gelbach JB, Miller DL (2008) Bootstrap-Based Improvements for Interence with Clustered Errors. *Rev Econ Stat* 90:414–427.

10. OECD (2013) *Agricultural Policy Monitoring and Evaluation 2013: OECD Countries and Emerging Economies* (Paris).